Modeling of Feedback and Rotational Stabilization of the Resistive Wall Mode in Tokamaks

M.S. Chu,[1] V.S. Chan,[1] M.S. Chance,[2] D.H. Edgell,[3] A.M. Garofalo,[4] A.H. Glasser,[5] S.C. Guo,[6] D.A. Humphreys,[1] T.H. Jensen,[1] J.S. Kim,[3] R.J. La Haye,[1] L. Lao,[1] G.A. Navratil,[4] M. Okabayashi,[2] F.W. Perkins,[2] H. Reimerdes,[4] H.E. St. John,[1] E. Soon,[7] E.J. Strait,[1] A.D. Turnbull,[1] M.L. Walker,[1] and S.K. Wong[1]

[1]General Atomics, P.O. Box 85608, San Diego, California 92186-5608
email: chum@fusion.gat.com
[2]Princeton Plasma Physics Laboratory, Princeton, New Jersey 08545
[3]FARTECH, Inc., San Diego, California 92121
[4]Columbia University, New York, New York 10027
[5]Los Alamos National Laboratory, Los Alamos, New Mexico 87545
[6]Consorzio RFX, Corso Stati Unit 4, Padova, 35127, Italy
[7]University of California, San Diego, 9500 Gilman Drive, La Jolla, California 92093-0417

Abstract. This paper describes the modeling of the feedback control and rotational stabilization of the resistive wall mode (RWM) in tokamaks. A normal mode theory for the feedback stabilization of the RWM has been developed for an ideal plasma with no toroidal rotation. This theory has been numerically implemented for general tokamak geometry and applied to the DIII-D tokamak. It is found that feedback with poloidal field sensors is superior to feedback with radial field sensors. The strength of the RWM that can be stabilized for a series of DIII-D equilibria are quantified. A general formulation is further developed for the feedback stabilization of tokamak with toroidal rotation and plasma dissipation. It has been used to understand the role of the external resonant field in affecting the plasma stability and compared with the resonant field amplification phenomenon observed in DIII-D. The effectiveness of a differentially rotating resistive wall in stabilizing the RWM has also been studied numerically. It is found that the maximum flow speed required is quite modest for a resistive wall with a long resistive wall time constant. It is orders of magnitude smaller than the required speed of plasma rotation. For a noncircular tokamak, a wide range of flow patterns have all found to be effective. The structure of the resistive wall mode predicted from ideal MHD theory has been compared with signals from various diagnostics. Simulation of the stabilization of the RWM in ITER-FEAT has been studied by using the MARS code coupled with the ONETWO transport code. It is also projected that 33 MW of negative neutral beam injection will be able to sustain plasma rotation sufficient to stabilize the RWM without relying on feedback.

1. Normal Mode Approach [1] to Feedback Stabilization

A practical tokamak fusion reactor must operate at high beta normal and high current [2]. This requires steady-state operation of the tokamak above the no wall β_N limit with sustained stabilization of the resistive wall mode (RWM) [3]. Plasmas in future reactors are expected to rotate with negligible rotation speed. Feedback stabilization of plasmas with no or negligible rotation is therefore of particular interest. In this case, the plasma dynamics is determined by a set of normal modes. The behavior of the feedback can then be prescribed completely from the properties of the normal modes.

Central to this approach is the consideration of the quadratic energy functional of the perturbed plasma displacement ξ in the plasma and the perturbed magnetic fields δB in the outside "vacuum" region:

$$\delta W_p + \delta W_v + D_w + \delta E_c = 0 \quad . \tag{1}$$

In Eq. (1), δW_p is the perturbed plasma potential energy, δW_v the perturbed vacuum energy, D_w the dissipation energy in the resistive wall, and δE_c the energy exchange between the feedback coil and the plasma resistive wall system. During the open loop operation $\delta E_c = 0$, Eq. (1) is self-adjoint and determines a set of normal modes, $\{\xi_i, \delta B_i\}$, with growth rates $\{\gamma_i\}$ and with D_w being the norm. This is an energy principle extended from that of the usual ideal MHD energy principle using D_w as norm replacing the plasma kinetic energy. Only one of these normal modes (the RWM) has been found to be unstable. The rest are stable

(damped) modes in which the resistive wall provides the dissipation. During the closed loop operation, the feedback currents and δE_c are non-zero and the requirement of Eq. (1) then determines that the amplitude of the normal modes $\{\alpha_i\}$ are determined by

$$\frac{\partial \alpha_i}{\partial t} - \gamma_i \alpha_i = E_i^c I_c \quad . \tag{2}$$

In Eq. (2), E_i^c is the excitation matrix which describes the excitation of the eigenmode ξ_i, δB_i by the feedback current I_c. The circuit equations for the currents I_c incorporate the feedback logic

$$\frac{\partial I_c}{\partial t} + \frac{1}{\tau_{cc'}} I_{c'} = G_{cl} F_{li}(\alpha_i) \quad . \tag{3}$$

In Eq. (3), $\tau_{cc'}$ is determined by the self and mutual inductances of the coils, F_{li} is the sensor matrix which measures the magnetic fluxes induced by the eigenmodes in the sensor loop l, and G_{cl} is the gain matrix. The stability of the feedback is completely described by Eq. (2) and (3) above and the closed loop feedback problem is reduced to a small set of coupled lumped circuit equations. This set of equations is, in general, non-self-adjoint. For feedback with a single array of sensors and a single array of feedback coils the stability may be studied by using the method of Nyquist diagram [4], and for multiple sensor arrays and multiple feedback coils the characteristic equations of Eqs. (2) and (3) have to be solved.

This approach has been applied to the DIII-D geometry shown in Fig. 1, with up to three bands (central midplane, upper, and lower) of external feedback coils. Shown in Fig. 2(a) is the Nyquist diagram for the stability of a set of equilibria with different β_N. For this set of equilibria, the plasma (which has not been optimized for its β value) is stable with no external wall at $\beta_N = 2.0$ and stable with the DIII-D wall infinitely conducting at $\beta_N = 2.6$. The curves are symmetric with respect to the horizontal axis. Only the upper half of each curve is shown. The Nyquist theorem demands that for plasma stability, the locus of the stability curve has to encircle the point (–1, 0). It is observed that the curves for $\beta_N = 2.06$ and 2.13 encircle (–1, 0),

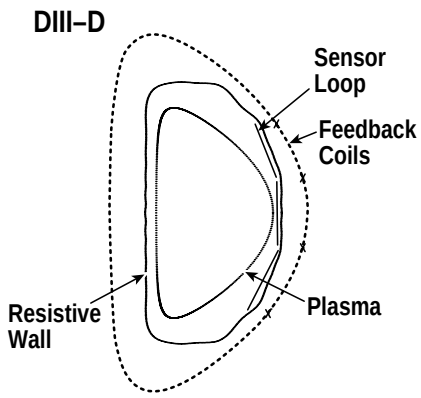

Fig. 1. Schematic of plasma, resistive wall, sensor loops and external feedback coil location in the poloidal cross section.

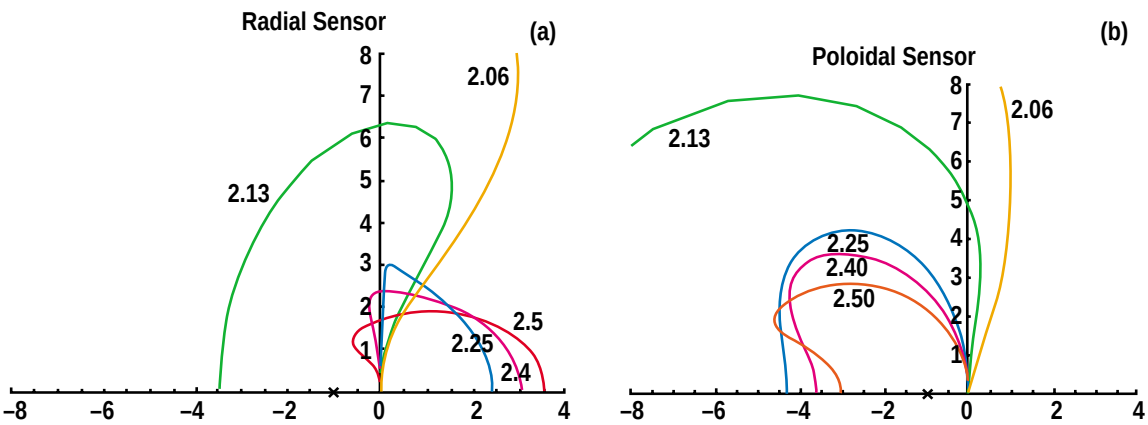

Fig. 2. Nyquist diagrams of transfer functions for equilibria with different β_N = (2.06, 2.13, 2.25, 2.4, 2.5). The curves are symmetric to the horizontal axis. Only the upper half of the curves are shown. Stable equilibria have curves which encircle (–1, 0). (a) Is for feedback with radial field sensors and (b) is for feedback with poloidal field sensors. It is seen that feedback with poloidal field sensors is much more effective than with radial field sensors.

showing that at these lower values of β_N the RWM is stabilized. Equilibria at higher β_N values are not stabilized. This is due to the coupling by the radial sensors of signals from the stable modes. Shown in Fig. 2(b) is the corresponding Nyquist diagram for feedback using poloidal field sensors. All the curves encircle (–1, 0), showing that the RWM is stabilized. This is due to the effective decoupling of the sensor signal and the non-detection of the perturbed radial magnetic field from that due to the stable modes. The effectiveness of using the radial sensors is studied further by using the method of solving the characteristic equations, with results summarized in Fig. 3. The strength of the RWM (growth rate normalized by the inverse resistive wall time, $\gamma\tau_w$, in absence of feedback and indicated by the curve which points to the scale on the right) for this set of equilibria is shown to be a strongly increasing function of plasma β. It is found that using the upper and lower bands of feedback coils can provide a substantial additional stabilization effect to the RWM. Using the radial sensors at the central midplane only, the strength of the RWM that can be stabilized is computed to be around $\gamma\tau_w = 1$. Together with the two upper and lower off-midplane bands, the strength of the RWM that can be stabilized (f=1) is up to a factor of 30 stronger. On the other hand, using the upper and lower bands only without the central band will limit the strength of the RWM that can still be stabilized to $\gamma\tau_w = 5$.

2. RWM Feedback With Inclusion of Plasma Rotation and Dissipation

In experiments in DIII–D, plasma rotation and dissipation have been found to stabilize the RWM even in the absence of feedback [5,6,7]. The nature of this dissipation has yet to be determined. Thus, it is important to have a formulation for studying the feedback stabilization in a plasma with rotation and dissipation. Here, we report on the continuation of the formulation that was set out in our previous work [8], taking into account our success from the normal mode approach. We note that the plasma dynamics relates the perturbed plasma magnetic field at the plasma boundary B_p to the complex Poynting flux S_p across the plasma vacuum interface.

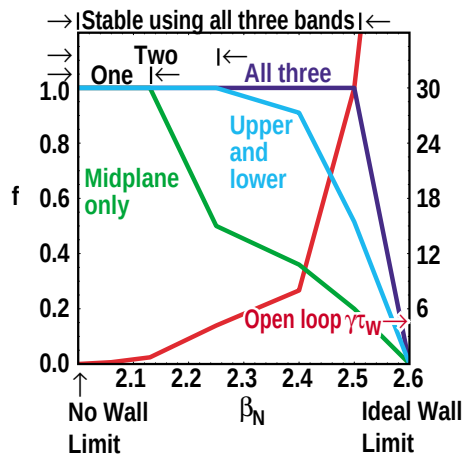

Fig. 3. *Effectiveness, f, of different feedback coil and radial sensor arrangements in stabilizing the plasma versus β; f is a measure of the completeness of suppression of the RWM normalized between f = 0 (no suppression) and f = 1 (complete suppression).*

The energy and momentum conservation across the plasma vacuum boundary allows us to relate B_p B_w, the perturbed magnetic field at the resistive wall,

$$B_p = \frac{-1}{\delta W_{Iw} + i\Omega D} C_{pw} B_w \quad . \tag{4}$$

In Eq. (4), δW_{Iw} is the perturbed energy for the ideal wall case, D is the dissipation matrix, and C_{pw} the reluctance matrix. From our previous work [8], we know that the magnetic perturbation on the resistive wall is driven by both the perturbation on the plasma surface and the external coil,

$$\tau_w \frac{\partial B_w}{\partial t} + MB_w = C_{wp} B_p - C_{wc} I_c \quad . \tag{5}$$

C_{wp} and C_{wc} are the corresponding reluctance matrices. Substitution of Eq. (5) into Eq. (4) gives a general equation for the excitation of the RWM by the external coils,

$$\tau_w \frac{\partial B_w}{\partial t} + \left[M + C_{wp} \frac{1}{\delta W_{Iw} + iD\Omega} C_{pw} \right] B_w = -C_{wc} I_c \quad . \tag{6}$$

In this equation we see that the dissipation on the wall, which is characterized by τ_w, and the dissipation in the plasma, which is characterized by iD, are described by different matrices. Also, the energy and the dissipation matrices are expected to be quite different and may not be diagonalized by the same eigenfunction. Without the external current, the behavior of the system is determined by the homogeneous equation with $I_c = 0$ in Eq. (6).

On the other hand, an external resonant field that is provided by the current source I_c will give rise to a response on the wall given by the solution of Eq. (6) with $\partial B_w/\partial t = 0$. If we assume that for the unstable mode, all the matrix elements can be approximated by constants, we obtain the following "lumped parameter" equation

$$\tau_w \frac{\partial B_w}{\partial t} + M \frac{1}{A} B_w = -C_{wc} I_c \quad , \tag{7}$$

where A is the "amplification factor" [9]. Note that $A = 1$ in the absence of plasma. In cylindrical approximation, we may further write

$$A = \frac{\delta W_{Iw} + i\Omega D}{\delta W_{nw} + i\Omega D} \quad . \tag{8}$$

δW_{nw} is the total (plasma + vacuum) potential energy without the external wall. By assuming reasonable behavior of this factor, the phase angle, the damping rate, and the amplitude of the response during the resonant field amplification experiment have been compared with experimental data [6] to show qualitative agreement. It is expected that a more detailed comparison should include more geometrical factors and the dependence of δW and D on the dissipation mechanism. We note that the present model only depends on the presence of a plasma damping mechanism for the resistive wall mode without specifically specifying it. In the future, we will utilize MHD codes such as MARS [10], with the inclusion of specific damping effects, to determine the matrices $\delta W_{Iw} + iD\Omega$ and compare with experimental observations.

3. Stabilization of the RWM With Nonuniform Wall Rotation, Mode Structure Study, and Prediction for ITER-FEAT

The RWM arises because the plasma perturbation excites a coherent skin current pattern on the resistive wall. This raises the question of whether a nonuniformly rotating wall with the aim of destroying the coherency of the perturbed skin current is more effective. We note that the present problem has been studied semi-analytically by Taylor *et al.* [11]. In their study, they neglected the poloidal wavelength of the perturbation. The present study is performed by modifying the MARS [10] code to allow a nonuniform toroidal rotation of the resistive wall. The normal component of the magnetic field δB_n on the resistive wall in this case is modified to satisfy the relationship

$$\frac{\partial \delta B_n}{\partial t} + in\Omega(l_w)\delta B_n = \hat{n} \cdot \nabla \times \delta B \quad . \tag{9}$$

In Eq. (13), the toroidal rotation frequency Ω is a function of its poloidal location l_w on the resistive wall, and $\hat{n}$ is a unit vector perpendicular to the resistive wall. We have applied the study to a noncircular tokamak with a D shape with inverse aspect ratio $R/a = 3$. We have found that the amount of shear flow required to stabilize the RWM is very small, with $\Omega\tau_w \sim 10$. For present day experiments, this speed is a factor of 10 lower than the corresponding

required plasma rotation speed. The flow speed has been found to scale inversely with the resistive wall time, indicating that the main stabilization mechanism is the destruction of the coherence of the mode structure of the penetrated flux. We have also found that stabilization is enhanced by the plasma dissipation. We have also found that the stabilization can be achieved by different flow patterns with comparable flow speeds. This is due to the fact that the resistive wall mode in tokamaks at high β is essentially toroidal in nature, with the toroidicity and pressure combining to couple neighboring poloidal harmonics.

The Mirnov fluctuation predicted from an ideal kink mode assumed to have penetrated the resistive wall has been compared with that predicted using matched filter analysis including the RWM and axisymmetric equilibrium motions [13]. The predicted electron temperature fluctuation derived from the ideal kink is also found to agree with observed ECE fluctuation at two times and two relative phases and amplitudes obtained from changes in Mirnov and saddle loop signals [14].

The presence of the RWM in the DIII-D experiment is identified through detailed comparison of the observed signals from the experiment with that anticipated from theory. The presence of a sufficiently large external error field causes the plasma to lose angular momentum and slow down. The plasma slowing resulting from these interactions is calculated from experiment in order to perform realistic simulations of the development of the RWM. For instance the uncorrected external error field has been found to cause anomalous angular momentum loss to the plasma at a rate comparable to the plasma energy confinement loss.

These comparisons are used as input for the simulation of RWM stability in the projected ITER-FEAT [12]. An AT type ITER-FEAT discharge scaled up from DIII-D shot 106029 was analyzed for stability to the RWM. The scaled up discharge has density ~0.93 n_{GW} with β_N H(89p) = 8.46, Q_{DT} =20.3, with 33 MW of 1 MeV tangential negative neutral beam injection. Primary and impurity ion densities and (equal) electron and ion temperature profiles were determined in such a way as to be consistent with the MHD equilibrium pressure and the fast alpha and neutral beam stored energy densities. It is shown that 33 MW of negative neutral beam injection is sufficient to maintain the central toroidal rotation speed at 2×10^4 rad/s using ion power balance diffusivity for the momentum diffusivity. The required central rotation speed for RWM stability is about 1.5×10^4 rad/s.

Acknowledgment

Work supported by U.S. Department of Energy under Grant Nos. DE-FG03-95ER54309, DE-FG03-99ER82791, DE-FG02-89ER53297, DE-FG03-95ER54294, and Contract Nos. DE-AC02-76CH03073 and DE-AC03-99ER54463.

References

[1] M.S. Chu, M.S. Chance, A. Glasser, and M. Okabayashi, Proc. of 28th Euro. Conf. on Plasma Physics and Controlled Fusion, Madeira, Portugal, 2002, Vol. 3 (European Physical Society, 2001) p. 601.
[2] R. Goldston and M. Kikuchi, Proc. of the 18th Fusion Energy Conf., Sorrento, Italy, 2002 (International Atomic Energy Agency, Vienna, 2002) Paper OV6/ITER/D.
[3] A.D. Turnbull, *et al.*, Nucl. Fusion **38**, 1467 (1998).
[4] Y.Q. Liu and A. Bondeson, Phys. Rev. Lett. **84**, 907 (2000).
[5] A.M. Garofalo, *et al.*., Phys. Plasmas **9**, 1997 (2002).
[6] M. Okabayashi, *et al.*, J. Plasma Fusion Res. Series, Vol. 5 (2002).
[7] E.J. Strait, *et al.*, this conference.
[8] M.S. Chance, M.S. Chu, M. Okabayashi, A.D. Turnbull, Nucl. Fusion **42**, 295 (2002).
[9] A.H. Boozer, Phys. Rev. Lett. **86**, 5059 (2001).
[10] A. Bondeson, *et al.*, Phys. Fluids B **4**, 1889 (1992).
[11] J.B. Taylor, J.W. Connor, C.G. Gimblett, H.R. Wilson, and R.J. Hastie, Phys. Plasmas **8**, 4062 (2001).
[12] L.L. Lao, *et al.*, this conference.
[13] D.H. Edgell, J.S. Kim, *et al.*, Rev. Sci. Instrum. **73**, 1761 (2002).
[14] A.M. Garofalo, A.D. Turnbull, M.E. Austin, *et al.*, Phys. Rev. Lett. **82**, 3811 (1999).